

# An Advanced Finite Element Model of IPMC

D. Pugal, H. Kasemägi, M. Kruusmaa, A. Aabloo  
Institute of Technology, Tartu University, Estonia

## ABSTRACT

This paper presents an electro-mechanical Finite Element Model of an ionic polymer-metal composite (IPMC) material. Mobile counter ions inside the polymer are drifted by an applied electric field, causing mass imbalance inside the material. This is the main cause of the bending motion of this kind of materials. All foregoing physical effects have been considered as time dependent and modeled with FEM. Time dependent mechanics is modeled with continuum mechanics equations. The model also considers the fact that there is a surface of platinum on both sides of the polymer backbone. The described basic model has been under development for a while and has been improved over the time. Simulation comparisons with experimental data have shown good harmony. Our previous paper described most of the basic model. Additionally, the model was coupled with equations, which described self-oscillatory behavior of the IPMC material. It included describing electrochemical processes with additional four differential equations. The Finite Element Method turned out to be very reasonable for coupling together and solving all equations as a single package. We were able to achieve reasonably precise model to describe this complicated phenomenon. Our most recent goal has been improving the basic model. Studies have shown that some electrical parameters of an IPMC, such as surface resistance and voltage drop are dependent on the curvature of the IPMC. Therefore the new model takes surface resistance into account to some extent. It has added an extra level of complexity to the model, because now all simulations are done in three dimensional domain. However, the result is advanced visual and numerical behavior of an IPMC with different surface characteristics.

**Keywords:** Electroactive polymers, EAP, IPMC, Finite Element method, Actuator, Coupled problem, Surface resistance.

## 1. INTRODUCTION

Electroactive polymer actuators have gained a lot of attention in many fields such as robotics and micro electronics. The advantages of EAP actuators are relatively simple mechanics and noiseless actuation. Additionally some EAPs, such as IPMCs,<sup>1</sup> are able to function in aqueous environments. Those qualities make the materials possible to use as so called artificial muscles. In this paper we consider three dimensional time dependent simulations of IPMC type materials with the Finite Element Method.

One of the most important qualities of IPMC materials is relatively large amplitude bending in response to electrical stimulation. An ion exchange polymer membrane, such as Nafion<sup>TM</sup>, Teflon<sup>TM</sup>, is covered with metal layers. The metal is typically platinum or gold. During the fabrication process the polymer membrane is saturated with certain solvent and ions. When voltage is applied to the metal electrodes, the ions start migrating due to the applied electric field. Migrating ions usually drag some solvent with them, causing expansion and contractions respectively near the surface layers. That in turn causes bending like actuation of IPMC sheet.

To simulate actuation of an IPMC sheet we need to solve coupled problems due to the complex nature of bending of an IPMC. Electrostatics, mass transfer and mechanical effects must be taken account to get a minimal functional base model which could predict actuation. Usually two dimensional time dependent model would be enough to get reasonable results. However, in this paper we consider three dimensional model of IPMC. This allows to take into account surface resistance changes for whole area of the metallic layer. Some authors<sup>2,3</sup> have already simulated mass transfer and electrostatic effects. We used similar approach in our model. Toi<sup>4</sup> has shown a Finite Element model including viscosity terms in transportation processes explicitly. The simulation is

---

Further author information: (Send correspondence to Alvo Aabloo)  
Alvo Aabloo: Email: alvo.aabloo@ut.ee

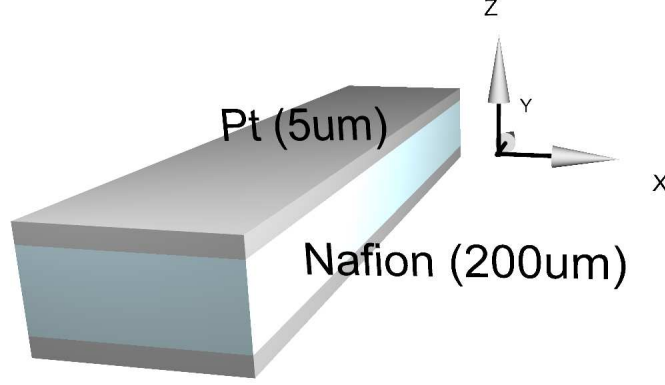


**Figure 1.** The IPMC strip, three-dimensional. The image is out of scale for illustrative purposes.

performed as time dependent and for three dimensions. However, the basis of the described model is a rectangular beam with 2 pairs of electrodes. Our approach for simulating mechanical bending is taking advantage of the numerical nature of FEM problems - we use continuum mechanics equations instead of analytical Euler beam theory which is more commonly used by authors.<sup>5,6</sup> By coupling equations from different domains, we get a three dimensional simple model for an IPMC muscle sheet. That allows us to build up a more complex model. In the last section of this article the variable surface resistance model is discussed.

## 2. BENDING SIMULATIONS

We have used Nafion<sup>TM</sup> 117, coated with thin layer of platinum in our experiments and therefore in theory. Mass transfer and electrostatic simulations are done only for backbone polymer. Continuum mechanics is taken into account for all domains, including the platinum coating. So there are two mechanical domains as shown in Figure 1.

All simulations are done for an IPMC strip of  $200\mu m$  thick polymer coated with  $5\mu m$  thick platinum, in a cantilever configuration - one end of the strip is fixed.

### 2.1. The base model

The cation migration in the polymer backbone is described by the Nernst-Planck equation, which covers migration and diffusion part. The equation is:

$$\frac{\partial C}{\partial t} + \nabla \cdot (-D\nabla C - z\mu FC\nabla\phi) = -\vec{u} \cdot \nabla C, \quad (1)$$

where  $C$  is concentration,  $\mu$  mobility of species,  $D$  diffusion constant,  $T$  absolute temperature,  $R$  universal gas constant,  $F$  Faraday constant,  $\vec{u}$  velocity,  $z$  charge number and  $\phi$  electric potential. The equations is solved only for cations as anions are fixed in the polymer backbone. As voltage is applied to the platinum electrodes, all free cations start migrating towards cathode, causing current in the outer electric circuit. As ions cannot move beyond the boundary of the polymer, local charge intensity starts to increase near the surface of the platinum electrodes, resulting in increase of electric field in the opposite direction to the applied one. This effect could be described by Gauss' Law:

$$\nabla \cdot \vec{E} = -\Delta\phi = \frac{F \cdot \rho}{\varepsilon}, \quad (2)$$

where  $\rho$  is charge density,  $\varepsilon$  is absolute dielectric constant and  $E$  is the strength of the electric field and can be also expressed as  $\nabla\phi = -\vec{E}$ . The formed steady state of the cations is shown in Figure 2. The corresponding electric field distribution is also shown in Figure 2.

Many authors like Shahinpoor<sup>7</sup> and Lee<sup>5</sup> have used cantilever beam equation to model bending of an IPMC strip in cantilever configuration. Though using Euler beam model provides us analytical solution for a static

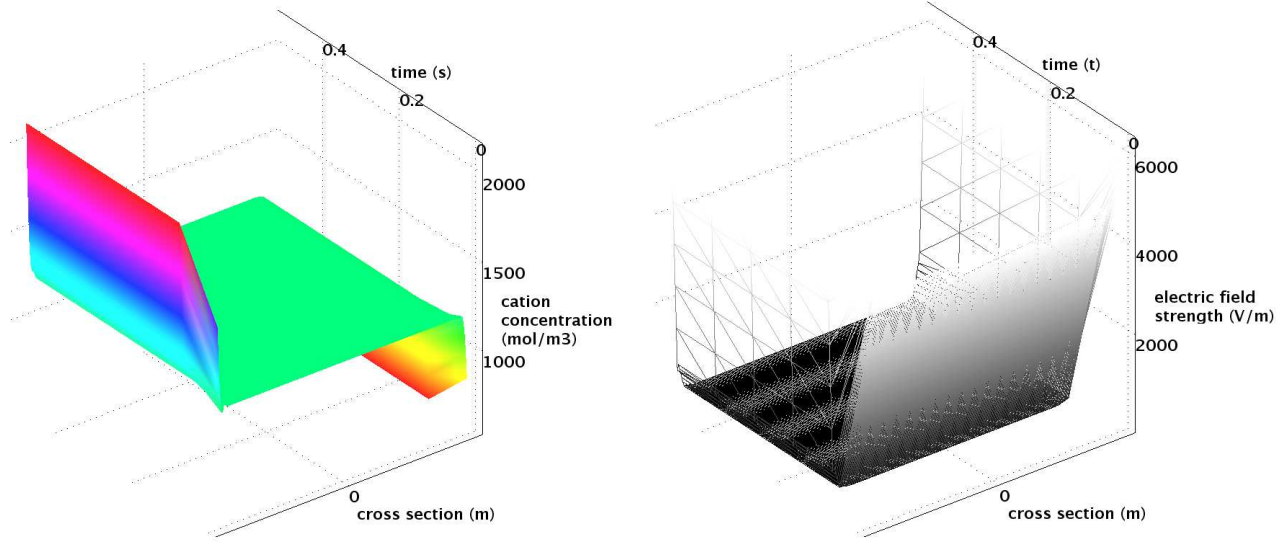


**Figure 2.** Cation concentration and electric field strength in an arbitrary cross section of an IPMC strip in time. The cross section length is  $200 \mu m$ , and the time is from 0 to 0.5 s.

configuration, the model described in this paper is dynamic. So more accurate results could be obtained by using continuum mechanics model with damping. The trade off is slower calculation speed, but the given model is not intended for using in real time simulations anyway. Importance of viscoelasticity has been brought out also by some other authors like Richardson<sup>8</sup> and Newbury.<sup>9</sup>

There are differences in charge distribution only in really thin boundary layers as shown in Figure 2. As many authors have concluded, only the boundary layers cause the bending.<sup>10</sup> The longitudinal force per unit cube in each point in the polymer of an IPMC is defined as follows:

$$\vec{F} = (A \cdot \rho + B \cdot \rho^2) \cdot \hat{y}, \quad (3)$$

where  $\rho$  is charge density and  $A$  and  $B$  are constants which could be fitted from different experiments.

To relate the force in Eq. 3 to the physical bending of an IPMC sheet, almost the same approach is used as in<sup>11,11</sup> Except this time all equations are solved in three dimensions. These equations are described in Comsol Multiphysics structural mechanics software package. Normal and shear strain are defined as

$$\varepsilon_i = \frac{\partial u_i}{\partial x_i}, \quad \varepsilon_{ij} = \frac{1}{2} \left( \frac{\partial u_i}{\partial x_j} + \frac{\partial u_j}{\partial x_i} \right), \quad (4)$$

where  $u$  is the displacement vector,  $x$  denotes a coordinate and indices  $i$  and  $j$  are from 1 to 3 and denote components correspondingly to x, y, or z direction. The general stress-strain relationship is

$$\sigma = D\varepsilon, \quad (5)$$

where  $D$  is  $6 \times 6$  elasticity matrix, consisting of components of Young's modulus and Poisson's ratio. The system is in equilibrium, if the relation

$$-\nabla \cdot \sigma = \vec{F}, \quad (6)$$

is satisfied. This is Navier's equation for displacement. The values of Young's modulus and Poisson's ratios, which are used in the simulations, are shown in Table 1.

As we are dealing with time dependent simulations, we have to describe the dynamics of actuation rather than statics. Besides, we also want to consider damping. The damping effect could be caused by material itself

and by the environment in which the IPMC is working. Therefore we use Rayleigh damping model to empirically describe the effect:

$$m \frac{d^2 u}{dt^2} + \xi \frac{du}{dt} + ku = f(t), \quad (7)$$

where the damping parameter  $\xi$  is expressed as  $\xi = \alpha m + \beta k$ . The parameter  $m$  is a mass,  $k$  is a stiffness and  $\alpha$  and  $\beta$  are correspondingly damping coefficients. By coupling Eq. (7) with Newton's equation, we get the the equation, which is describes the dynamics of an IPMC strip:

$$\rho \frac{\partial^2 \vec{u}}{\partial t^2} - \nabla \cdot \left[ c \nabla \vec{u} + c \beta \nabla \frac{\partial \vec{u}}{\partial t} \right] + \alpha \rho \frac{\partial \vec{u}}{\partial t} = \vec{F}. \quad (8)$$

The origin of the equation is covered in<sup>11</sup> and also in Comsol Multiphysics manual.

So far we have described the base model, which is usable in both two dimensional and three dimensional modeling. The parameters for given equations Eq. (1) - Eq. (8) are given in Table 1. The illustrative example of bending is shown in Figure 3.

| Variable      | Value               | Dimension                 | Comment   |
|---------------|---------------------|---------------------------|---|
| $D_{cation}$  | $2 \cdot 10^{-9}$   | $\frac{m^2}{s}$           | Diffusion coefficient of cations, e.g Na+.  |
| $\varepsilon$ | $3.8 \cdot 10^{-5}$ | $\frac{F}{m}$             | From capacitance measurement of an IPMC.  |
| $\mu$         | $8 \cdot 10^{-13}$  | $\frac{mol \cdot s}{kg}$  | From Nernst-Einstein relation $\mu = \frac{D}{R \cdot T}$ where $T = 293K$ , $R = 8.31 \frac{J}{mol \cdot K}$ . |
| $Y_N$         | $50 \cdot 10^6$     | $Pa$                      | Young modulus of Nafion <sup>TM</sup> .   |
| $Y_{Pt}$      | $169 \cdot 10^9$    | $Pa$                      | Young modulus of platinum.  |
| $\rho_N$      | 2600                | $\frac{kg}{m^3}$          | Density of Nafion <sup>TM</sup> .   |
| $\rho_{Pt}$   | 21500               | $\frac{kg}{m^3}$          | Density of platinum.  |
| $A$           | $5 \cdot 10^5$      | $\frac{N \cdot m}{C}$     | A constant in Eq. (3).  |
| $B$           | $3 \cdot 10^4$      | $\frac{N \cdot m^4}{C^2}$ | A constant in Eq. (3).  |
| $\alpha$      | 1                   | $\frac{1}{s}$             | Mass damping parameter.   |
| $\beta$       | 0.5                 | $s$                       | Stiffness damping parameter.  |

**Table 1.** Simulation values of the base model.

### 2.1.1. Meshing in three dimensional domain

Meshing in a three dimensional domain is not as straightforward as it is for two dimensions. There are couple of things which should be taken into account. First of all, two dimensions of an IPMC sheet are relatively large (width and length are in range of centimeters) but the thickness is really small, much less than a millimeter. In addition, the thickness consists of three layers - a polymer backbone and two layers of metal coating which are considered as separate domains. Therefore the tetrahedral mesh really cannot be used over all the domains as the degrees of freedom for calculations would be unreasonably large. That is why the mapped meshing technique is used. Instead of tetrahedral fine mesh, the rectangular coarser mesh is created. The coarseness of the mesh is larger in the areas, where physical variables do not tend to change very rapidly. For instance the concentration of cations is rather smooth function in the middle of polymer backbone. Therefore areas around the surface layers contain finer mesh. As the problem is solved in number of physical domains, it is not really straightforward to analytically determine the optimal mesh size. Instead trial and error method could be used and after performing some simulations, the smoothness of the results could help to determine the optimal size of the mesh for future simulations. Example of a mesh could be seen in Figure 4.

### 2.2. Extended model

The model described in the previous section is good for both two dimensional and three dimensional modeling. However, solving the base model in three dimensional domain does not give us any kind of extra information. Instead it adds some complexity such as more complicated meshing and increased solving times. The real

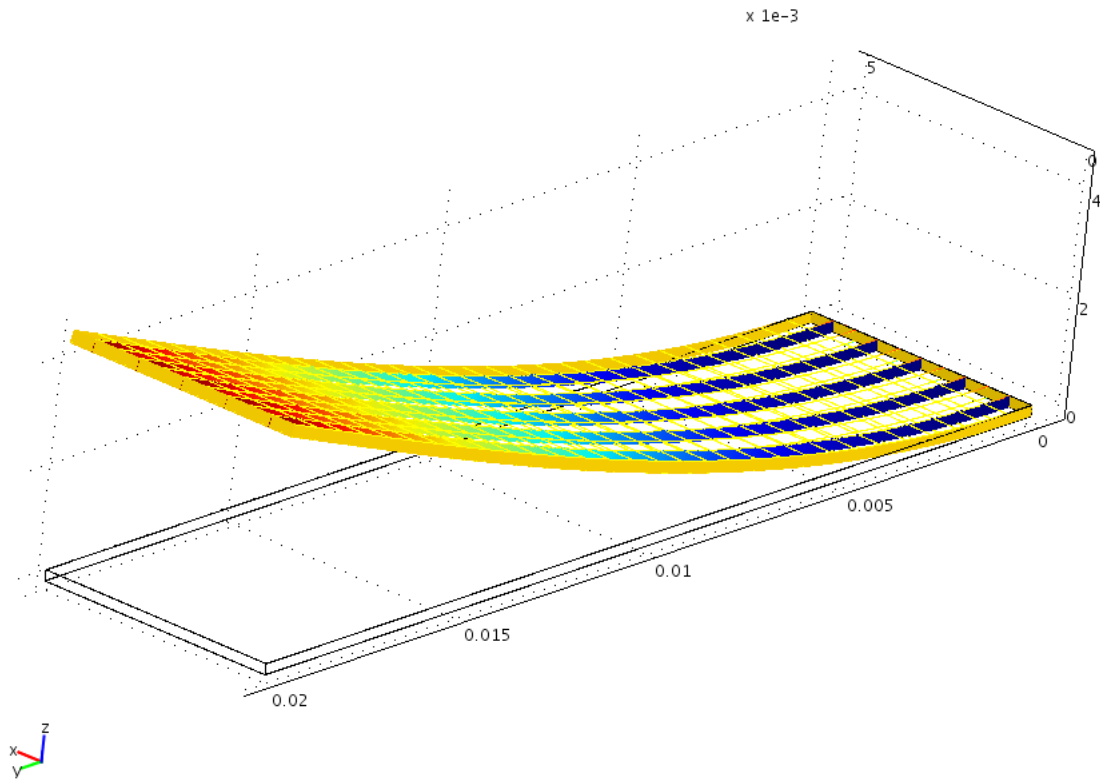


**Figure 3.** Example of three dimensional bending of an IPMC sheet. The length of the strip is  $2\text{cm}$ , the width is  $0.5\text{cm}$  and the bending amplitude is approximately  $4\text{mm}$ .

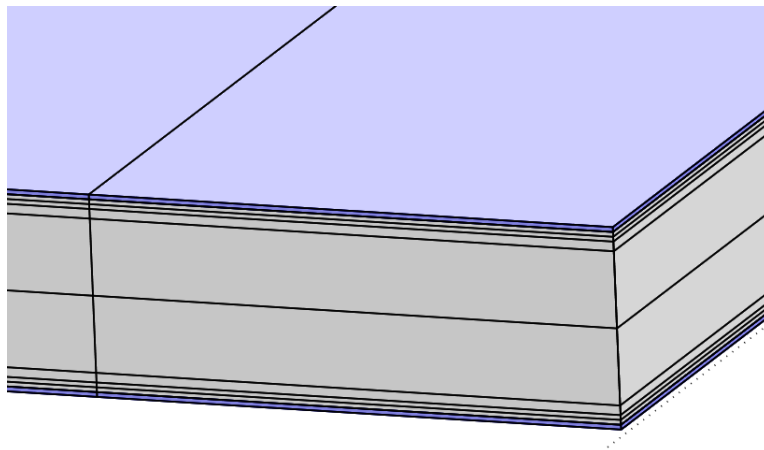


**Figure 4.** Meshing of an IPMC strip. One corner of the strip is shown. Notice the coarse mesh in the middle of the IPMC but fine mesh near the boundaries.

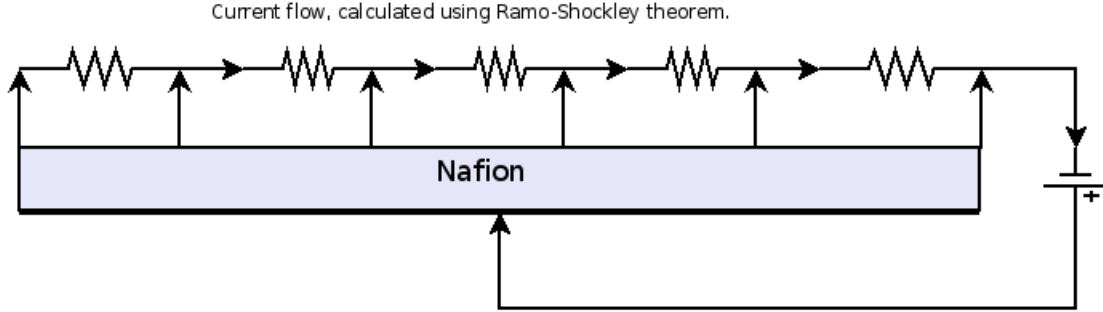


Figure 5. The conceptual diagram of the model.

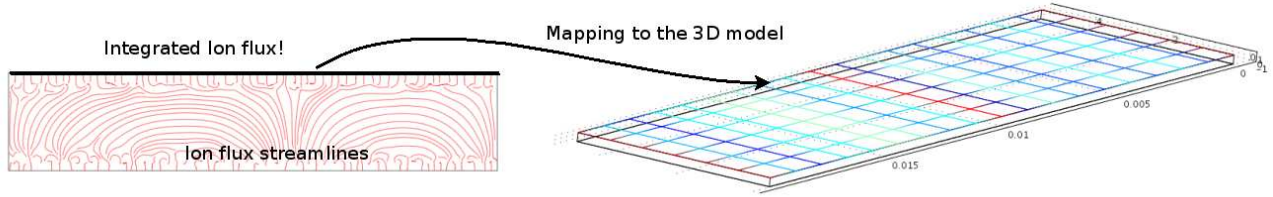


Figure 6. Mapping the calculated current to the three dimensional model.

usefulness of the third dimension comes, when the model takes into account also the surface resistance of the electrodes.

The surface resistance is an interesting characteristic of an IPMC strip. Besides of being different for different IPMC sheets, it tends to depend on the curvature of the IPMC strip.<sup>12</sup> On the other hand, the surface resistance is the parameter which could be rather easily changed. For instance it is possible to make some areas of the muscle sheet less conductive. That's the place where 3 dimensional model could be useful.

The idea of the extended model is to put together part of the electrical model, which includes active resistances and the model described in the previous section. It means that the cation transportation and continuum mechanics is coupled to the currents in the surface layers.

### 2.2.1. Currents in the surface layers

An IPMC strip connected to an external power source forms an electric circuit. There are roughly two types of conduction mechanisms in the circuit: electron conduction in the outer part of the circuit and ion migration in the IPMC. Even though the ions move only inside the polymer backbone, there is a connection between current in outer circuit and displacement of the ions. The theorem which is more often used in plasma physics,<sup>13</sup> is called Ramo-Shockley theorem. The theorem connects movement of charged particles in confined space to the current in connected electric circuit. The theory have been for instance used for modeling ion channels.<sup>14</sup> The general equation is:

$$I = \frac{1}{V} \sum_i q_i \times W(\vec{r}_i)_i \vec{v}_i, \quad (9)$$

where  $j$  is the index of a particle,  $q$  is the charge, and  $v$  is the velocity of a particle.  $W$  corresponds to a electric field which would exist without any charged particles present.<sup>14</sup> By using Eq. (9), we can calculate the current flowing in an electrode and therefore also voltage in the surface layer. The conceptual diagram is shown in Figure 5. only Notice that there are number of resistors shown in the figure. Those resistors resemble the metallic electrode. The current model considers voltage drop only at the one side of the IPMC sheet - the side which stretches during the actuation - as the resistance of this electrode is bigger.<sup>12</sup>

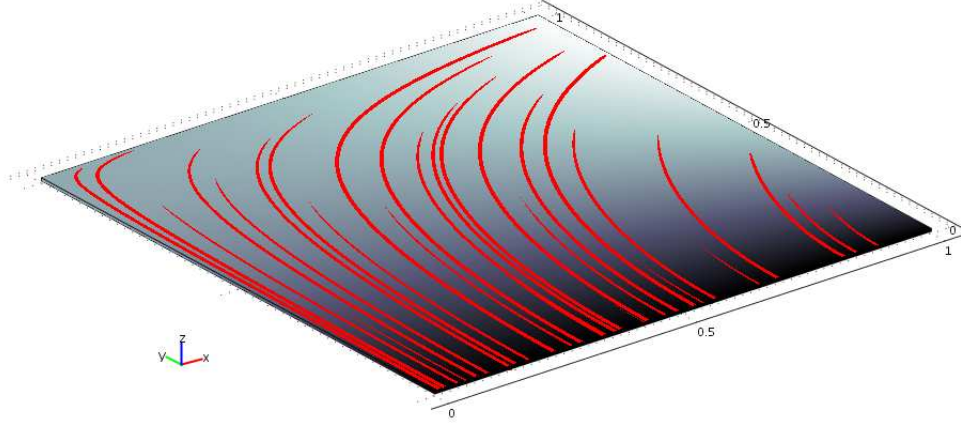


**Figure 7.** An electrode surface with the area of one square millimeter. The  $0V$  is applied to the edge  $y = 0$ . There is a current inflow from the bottom surface, which resembles the connection with polymer backbone. The conductivity of the electrode is maximum at  $x = 0$  and decreases to zero at  $x = 1$ . The plot shows the voltage distribution - voltage of the lighter areas is greater than voltage of the darker areas. The lines show the constant current density in the electrode.

### 2.2.2. Simulation details

The simulation of proposed model coupled with the base model is rather complex problem. The complexity comes from the fact that considering the surface resistance gives an extra variable which controls the applied voltage. At the same time the applied voltage controls the current inside the polymer. However, there are ways to simplify the model by means of reducing solution time. One way to optimize is to calculate the current flow in two dimensional domain - two dimensional polymer - and then extend the solved value to the three dimensional model. The conceptual diagram is shown in Figure 6. As the ions migrate, we know the total flux with unit  $mol/(m^2s)$ . By using the equation

$$I = \frac{F}{d} \int_0^d \vec{j} \cdot d\vec{z}, \quad (10)$$

where  $d$  is the distance between electrodes and  $\vec{j}$  is the migration current,  $F$  is Faraday constant, it is possible to calculate the current  $I$  in the electrodes.

The given model is able to calculate surface currents and voltages at the initial moment. So the time dependency is yet to come. The illustrative plot of the voltage distribution on the surface and the current streamlines in the surface is shown in Figure (7). The figure shows how the voltages and currents could possibly distribute in the electrode surface during the first moments of actuation. As it could be seen, the voltage distribution is not uniform at all, which is also supported by the measurements.<sup>15</sup> Preliminary data and simulations show that the given theory should be develop further to obtain more sophisticated time dependent three dimensional model of an IPMC.

## 3. CONCLUSIONS

We have developed a base model to model the simple physical processes such as ion migration and electric field change in an IPMC. In this paper we have extended the base model to three dimensions. Some improvements in meshing techniques have been necessary to be able to solve the three dimensional model within reasonable time. To get the full use of the three dimensional model, we introduced the mechanism for calculating currents inside the electrodes as a result of ion movement. The used theory is Ramo-Shockley theorem mostly know in other fields of physics. However, the theorem could be applicable also for an IPMC to estimate currents and therefore voltage drops inside the electrodes. In this paper we have shown only the simple simulations of electrode currents, but the given theory could be extended further to get a more sophisticated model of a three dimensional IPMC actuator.

## 4. FUTURE WORK

Future work will be extending the given model, possibly using some electric circuit modeling coupled with calculations of Ramo-Shockley theorem to predict the currents inside the electrodes of an IPMC.

## ACKNOWLEDGMENTS

We want to acknowledge the support from Estonian Science Foundation, grant #6763. Also we acknowledge Estonian Archimedes Foundation for travel support of Deivid Pugal to San Diego.

## REFERENCES

1. M. Shahinpoor and K. Kim, "Ionic polymer-metal composites. I- Fundamentals," *Smart Materials and Structures* **10**(4), pp. 819–833, 2001.
2. T. Wallmersperger, B. Kröplin, and R. Gülch, "Coupled chemo-electro-mechanical formulation for ionic polymer gels—numerical and experimental investigations," *Mechanics of Materials* **36**(5-6), pp. 411–420, 2004.
3. S. Nemat-Nasser and S. Zamani, "Modeling of electrochemomechanical response of ionic polymer-metal composites with various solvents," *Journal of Applied Physics* **100**(6), pp. 64310–64310, 2006.
4. Y. Toi and S. Kang, "Finite element analysis of two-dimensional electrochemical–mechanical response of ionic conducting polymer–metal composite beams," *Computers and Structures* **83**(31-32), pp. 2573–2583, 2005.
5. S. Lee, H. Park, and K. Kim, "Equivalent modeling for ionic polymer–metal composite actuators based on beam theories," *Smart Mater. Struct* **14**, pp. 1363–8, 2005.
6. T. Wallmersperger, D. J. Leo, and C. S. Kothera, "Transport modeling in ionomeric polymer transducers and its relationship to electromechanical coupling," *Journal of Applied Physics* **101**(2), p. 024912, 2007.
7. M. Shahinpoor, "Electro-mechanics of ionic-elastic beams as electrically-controllable artificial muscles," *Artificial Muscle Research Institute, School of Engineering & School of Medicine, University of New Mexico, Albuquerque, New Mexico* **87131**.
8. R. Richardson, M. Levesley, M. Brown, J. Hawkes, K. Watterson, and P. Walker, "Control of Ionic Polymer Metal Composites," *IEEE/ASME Transactions on Mechatronics* **8**(2), p. 245, 2003.
9. K. Newbury, *Characterization, Modeling, and Control of Ionic Polymer Transducers*. PhD thesis, Virginia Polytechnic Institute and State University, 2002.
10. S. Nemat-Nasser and J. Li, "Electromechanical response of ionic polymer-metal composites," *Journal of Applied Physics* **87**(7), p. 3321, 2000.
11. D. Pugal, A. Kim, J. K. and Punning, K. H., M. Kruusmaa, and A. Aabloo, "A Self-Oscillating Ionic Polymer-Metal Composite Bending Actuator," *Journal of Applied Physics* , in review.
12. A. Punning, M. Kruusmaa, and A. Aabloo, "A self-sensing ion conducting polymer metal composite (IPMC) actuator," *Sensors & Actuators: A. Physical* **136**(2), pp. 656–664, 2007.
13. P. Paris, M. Aints, M. Laan, and T. Plank, "Laser-induced current in air gap at atmospheric pressure," *Journal of Physics D: Applied Physics* **38**(21), pp. 3900–3906, 2005.
14. W. Nonner, A. Peyser, D. Gillespie, and B. Eisenberg, "Relating Microscopic Charge Movement to Macroscopic Currents: The Ramo-Shockley Theorem Applied to Ion Channels," *Biophysical Journal* **87**(6), pp. 3716–3722, 2004.
15. A. Punning, M. Kruusmaa, and A. Aabloo, "Surface resistance experiments with IPMC sensors and actuators," *Sensors & Actuators: A. Physical* **133**(1), pp. 200–209, 2007.